

Monitoring the growth of III-nitride materials by plasma assisted molecular beam epitaxy employing diffuse scattering of RHEED

Cite as: J. Vac. Sci. Technol. B **38**, 014007 (2020); <https://doi.org/10.1116/1.5124048>

Submitted: 10 August 2019 . Accepted: 25 November 2019 . Published Online: 18 December 2019

Sayantani Sen, Suchismita Paul, Chirantan Singha, Anirban Saha, Alakananda Das, Pushan Guha Roy, Pallabi Pramanik, and Anirban Bhattacharyya



View Online



Export Citation



CrossMark

ARTICLES YOU MAY BE INTERESTED IN

[Nanoscale etching of perovskite oxides for field effect transistor applications](#)

Journal of Vacuum Science & Technology B **38**, 012201 (2020); <https://doi.org/10.1116/1.5122667>

[Temperature-dependence of Cl₂/Ar ICP-RIE of polar, semipolar, and nonpolar GaN and AlN following BC₁₃/Ar breakthrough plasma](#)

Journal of Vacuum Science & Technology A **38**, 013001 (2020); <https://doi.org/10.1116/1.5123787>

[Spectral ellipsometry of monolayer transition metal dichalcogenides: Analysis of excitonic peaks in dispersion](#)

Journal of Vacuum Science & Technology B **38**, 014002 (2020); <https://doi.org/10.1116/1.5122683>

HIDEN
ANALYTICAL

Instruments for Advanced Science

Contact Hiden Analytical for further details:

W www.HidenAnalytical.com
E info@hiden.co.uk

[CLICK TO VIEW](#) our product catalogue



Gas Analysis

- dynamic measurement of reaction gas streams
- catalysis and thermal analysis
- molecular beam studies
- dissolved species probes
- fermentation, environmental and ecological studies



Surface Science

- UHV/TPD
- SIMS
- end point detection in ion beam etch
- elemental imaging - surface mapping



Plasma Diagnostics

- plasma source characterization
- etch and deposition process reaction kinetic studies
- analysis of neutral and radical species



Vacuum Analysis

- partial pressure measurement and control of process gases
- reactive sputter process control
- vacuum diagnostics
- vacuum coating process monitoring



Monitoring the growth of III-nitride materials by plasma assisted molecular beam epitaxy employing diffuse scattering of RHEED

Cite as: J. Vac. Sci. Technol. B 38, 014007 (2020); doi: 10.1116/1.5124048

Submitted: 10 August 2019 · Accepted: 25 November 2019 ·

Published Online: 18 December 2019



Syantani Sen,¹ Suchismita Paul,¹ Chirantan Singha,¹ Anirban Saha,² Alakananda Das,² Pushan Guha Roy,² Pallabi Pramanik,³ and Anirban Bhattacharyya^{2,a)}

AFFILIATIONS

¹Centre for Research in Nanoscience and Nanotechnology, University of Calcutta, Kolkata 700106, India

²Institute of Radio Physics and Electronics, University of Calcutta, Kolkata 700009, India

³Department of Electronics and Telecommunication Engineering, Indian Institute of Engineering Science and Technology, Shibpur, Howrah 711103, India

^{a)}Electronic mail: anirban.rpe@caluniv.ac.in

ABSTRACT

AlGa_N alloys find important applications in UV emitters and detectors, as well as in high-power high-frequency electronics. While reflection high energy electron diffraction (RHEED) is a standard technique for *in situ* monitoring of the growth of AlGa_N alloys by plasma assisted molecular beam epitaxy, this paper investigates a new mode of its application. During the growth of AlGa_N alloys, the ratio of the group III (Al + Ga) to group V (active nitrogen) adatoms critically controls the materials property of AlGa_N films and is optimal within a very narrow window of operation. Moreover, this ratio is dependent in a complex fashion on various growth parameters, including substrate temperature, and is difficult to determine quantitatively in real time. This paper provides a method to estimate that important parameter. This can be carried out through the capture of the RHEED image from the fluorescent screen using an inexpensive video camera setup and a simple analysis procedure. While most RHEED analyses focus on the diffraction pattern, e.g., the line spacing, this work quantifies diffused scattering of the electron beam from a metallic layer that forms on the top of the growth surface during deposition under excess group III conditions, which is typically employed during growth. Two alternate methods for data analysis have been explored and compared. The results indicate that this process can qualitatively trace the variation of the thickness of the thin metallic layer, and hence the group III to group V flux ratio, for different substrate temperatures. This technique being simple, fast, and cost-effective can be incorporated into standard MBE systems for real-time *in situ* characterization of AlGa_N alloys.

Published under license by AVS. <https://doi.org/10.1116/1.5124048>

I. INTRODUCTION

The growth of semiconductors by molecular beam epitaxy (MBE) traditionally benefitted over competing deposition techniques due to the presence of *in situ*, real-time monitoring systems. Reflection high energy electron diffraction (RHEED) is a standard characterization tool currently employed in most commercial MBE systems. Several commercial entities have produced software and hardware monitoring systems that contain image acquisition and analysis capabilities. Such systems routinely analyze features such as linewidth and line spacing and generate parameters that quantify crystal quality and lattice constants,

which allow real-time compositional analysis. Besides these, RHEED intensity oscillations also generate information about the growth rate for certain growth modes.¹

A. Reflection high energy electron diffraction (RHEED)

Early works on the RHEED image analysis generated information about the crystal orientation, for example, cubic versus hexagonal symmetries.² Real-time analysis of RHEED patterns indicated that the growth kinetics and the surface configurations generated are closely interlinked.³ Streaky RHEED patterns were obtained when the growth of GaN was carried out under excess group III,

while spotty features, indicating rough surfaces, were a signature of group V-rich conditions.² The growth of wurtzite GaN can either be gallium polar or nitrogen polar, and a link has been established between the polarity of the material to the type of buffer layers employed.⁴ GaN buffers grown at lower substrate temperature typically lead to N-polar material, while AlN buffer layers deposited at higher temperature lead to Ga polarity.⁵ Furthermore, the stability of the two surfaces is widely different under nitrogen exposure. Thus, the evolution of the RHEED pattern of GaN surfaces exposed to active nitrogen has been employed as an indicator of the crystal polarity.⁶ The polarity has also been tested by the RHEED surface reconstruction pattern. A 2×2 reconstruction pattern observed from a GaN surface upon exposure to active nitrogen at high temperatures typically indicates a Ga polarity.⁷ On the other hand, an unreconstructed RHEED pattern at high temperature followed by a 3×3 pattern observed upon cooling down the sample to ~ 400 °C indicates a nitrogen polarity.⁵ This real-time monitoring of thin films of GaN by RHEED has been instrumental in the development of various electronic and optoelectronic devices based on III-nitride materials by MBE.

In the field of RHEED image analysis, the intensity of the RHEED image has been measured by using a scintillator and a photomultiplier tube⁸ or by magnetically deflecting electrons through a hole in the RHEED screen onto a collimating aperture and a Faraday cup where a retarding field has been applied.⁹ In later years, high quality video camera systems have been employed in order to record the RHEED image from the fluorescent screen and subsequently analyze it.^{10,11} Software is also freely available to convert RHEED patterns to the corresponding 2D reciprocal lattice image. For current commercial RHEED analysis systems, the image is recorded using a high-resolution CCD camera with high frame rates, large pixel sizes along with sophisticated image acquisition and analysis software. However, the information obtainable from the RHEED image goes beyond the pattern and line spacing, and this paper investigates RHEED diffuse scattering as a parameter for real-time *in situ* monitoring of the growth of III-nitride materials by plasma assisted molecular beam epitaxy (PA-MBE).

B. Growth of III-nitride by PA-MBE

The growth of III-nitride alloys, such as AlGaIn, has been under focus for a long time due to their various applications in ultraviolet emitters¹² and detectors,¹³ as well as in high-power high-frequency electronics.¹⁴ These materials, when grown by PA-MBE, show very interesting features, such as high internal quantum efficiencies for UV emission,¹⁵ very large mobility-lifetime product for detectors,¹⁶ and relatively high levels of n-type¹⁷ and p-type doping.¹⁸ However, important material parameters such as crystal quality, surface morphology, mobility of carriers, background impurity levels, efficiency of doping, carrier recombination and lifetimes, etc., depend strongly on the growth parameters, such as substrate temperature¹⁹ and the group III to group V flux ratio.²⁰ A smooth surface morphology for GaN grown by PA-MBE is typically obtained under excess group III conditions of growth.²¹ Dislocation density annihilation, on the other hand, is enhanced under the stoichiometric regime.²² P-type doping is most efficient under large excess Ga conditions.¹⁸

This dependence is even more pronounced for AlGaIn alloys. For growth of AlGaIn alloys under excess group III conditions, the alloy composition depends on the ratio of the active nitrogen to the arrival rate of Al. However, for growth under excess group V, it depends on the ratio of the arrival rate of the metals—Al and Ga. Growth of AlN can only be carried out in a small parameter window for PA-MBE. Excess group V leads to polycrystalline films, while excess group III conditions lead to coverage of the surface with metallic Al which halts further deposition. Depending on the small variation of the group III to group V flux ratio, one can obtain rough but continuous thin films, smooth films, AlN nanorods, or embedded Al particles.^{21,23,24} Determining the group III to group V flux ratio accurately is made complicated by the fact that it depends on many parameters like the arrival rate of the metal atoms and their desorption rate, the latter depending on substrate temperature, and the arrival rate of active nitrogen, which depends on the RF plasma power, flow rate, and chamber pressure. These are difficult to calculate *a priori* and can drift significantly during the deposition process. Thus, an *in situ*, real-time estimation of the group III to group V flux ratio is vital for an accurate and repeatable growth process. The study of binary AlN and GaN has been reported using RHEED intensity as an analytical tool, and the various growth regimes have been identified from the *in situ* intensity evolution. High sensitivity 22-bit cameras have been employed to control the growth of GaN doped with Mg in a closed loop fashion.^{25,26}

II. EXPERIMENTAL METHODS

A. MBE growth

In this work, growth of Ga-polar GaN thin films has been carried out using a VEECO Gen 930 MBE system. Sapphire substrates were employed for this work. The substrates were outgassed at 400 °C in the preparation chamber of the system till a vacuum level of 1×10^{-9} T was achieved, before introduction into the growth chamber. The MBE system is equipped with standard effusion cells for Ga and Al and an RF source for nitrogen activation. The 2-in. substrate was mounted on the growth stage and maintained at 800 °C initially. The plasma power used for the growth of the film was 350 W, and the nitrogen flow used was 1.7 sccm. In order to promote uniformity, the substrate was rotated at a rate of 3 RPM. A Staib Instruments 15 KV RHEED gun was employed for real-time analysis. Molly® Growth Control software was used to interface the MBE system.

B. RHEED image capture and analysis

The schematic of the MBE along with the RHEED image capture system is presented in Fig. 1. The diffraction pattern as observed on the fluorescent screen was captured by a video camera (Moticam). The pixels resolution was 916×686 , and the pixel size was $1.67 \times 1.67 \mu\text{m}^2$. The camera was interfaced using its associated software, and the video was recorded in the .avi format at 27 FPS. The data were transferred directly to a central processing unit using a USB 2 data transfer line. It should be noted that this is of a significantly lower configuration compared to standard commercial RHEED acquisition systems.

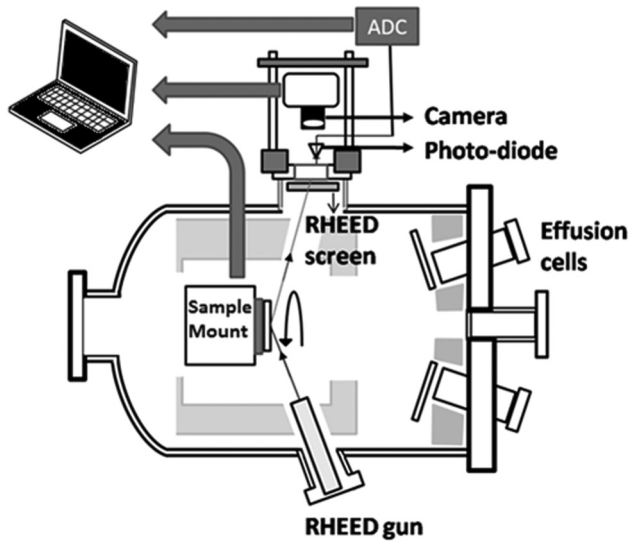


FIG. 1. Schematic of the MBE system along with the camera setup in order to capture the RHEED image.

Post growth, the video file captured during a growth segment was analyzed using freely available software. During the growth, the substrate rotates at a rate of 3 RPM for the sake of sample uniformity. Thus, various crystal planes are oriented in a time periodic fashion, of which the pattern corresponding to the a-plane [11–20] has been considered for analysis during this work. The appropriate frames have been captured using free software and analyzed using ImageJ. It should be clarified that no additional preprocessing has been carried out. From the captured images (in the form of JPG files), the intensity (pixel value) is plotted along a line perpendicular to the RHEED streaks typically obtained from flat surfaces. The intensity variation of this “plot profile” has been considered a parameter during this work. A second parameter also investigated is the overall pixel intensity distribution of the entire RHEED image, in the form of a histogram. While additional information such as the width and spacing of the streaks requires further data processing, we have selected these two parameters as they can be obtained very fast and, therefore, are appropriate for real-time analysis.

III. RESULTS AND DISCUSSION

It has been previously stated that for PA-MBE growth of GaN and related materials, the group III to group V ratio is an important growth parameter^{20,27–29} that controls many material properties. The amount of group III, that is, Ga, Al, or In, may be the same as that of group V, that is active nitrogen, leading to stoichiometric deposition conditions. However, most growth takes place under a III/V ratio greater than unity, for reasons listed previously. Under the circumstance, there is a thin layer of metal on the growth surface during the deposition period. This is reflected in the RHEED pattern, as this metallic layer scatters incoming electrons, and masks the crystal surface. The electrons that penetrate this layer to

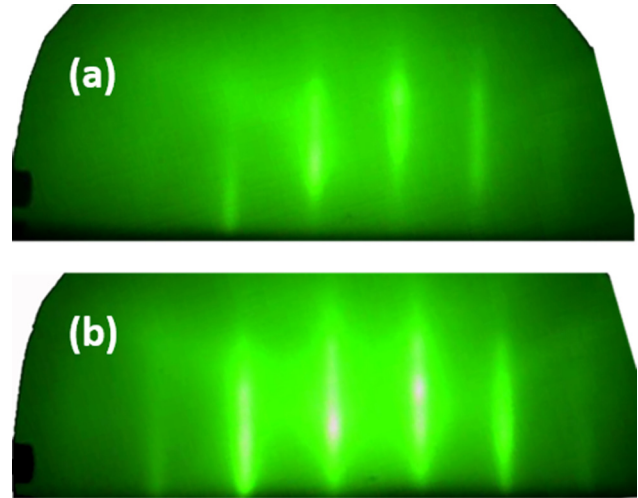


FIG. 2. RHEED image taken during Ga metal deposition (a) and after reaction of the deposited metal with nitrogen plasma (b).

reach the surface are diffracted, and these electrons again have to travel through a metallic layer to emerge from the surface, before it can reach the fluorescent screen. The overall impact of the metallic layer, therefore, is to create a pattern that is diffuse and dim. This can be seen in Fig. 2(a) which was taken during growth of a GaN thin film under excess group III conditions. If the metallic shutters, in this case for Ga, are closed and the surface is kept under active nitrogen, this metallic layer is consumed over time and the RHEED pattern changes to that given in Fig. 2(b). As can be observed, the pattern remains qualitatively the same, with no variation in nature or line spacing, but has much better contrast.

The thickness of this metallic layer is difficult to estimate by calculating the arrival rates of active species but is critical in many applications. We have developed a technique for the quantitative analysis of this important parameter through analysis of the RHEED diffraction pattern evolution.

A. Analysis of RHEED images obtained from GaN deposition

Growth of GaN films was carried out on to sapphire wafers for this work. The thin films were grown in this system using a modified metal enhanced epitaxy process. In this technique, the substrate is exposed to the nitrogen plasma throughout the growth, while the Ga shutter is opened intermittently. After depositing Ga on the growth surface for a specific duration of time, the Ga shutter is closed. Some part of the metal that has not reacted with nitrogen till then remains on the growth surface as a metallic film and makes the RHEED pattern diffused. This accumulated metal is allowed to react completely with the incoming nitrogen plasma. Once all of the accumulated metal has been consumed, the RHEED turns sharp and bright. Once this has occurred, the metal shutters are opened again for further growth.

One entire cycle, comprising the steps of (i) GaN deposition under group III-rich conditions, (ii) closing of Ga shutter keeping the nitrogen shutter open, and (iii) reaction of accumulated metal with active nitrogen, was recorded in the RHEED video. Frames showing the same plane (a-plane) were captured from this video, and the corresponding JPG files were analyzed as explained previously. The results are shown in Fig. 3.

Figure 3(a) shows the plot profile, that is, the spatial distribution of intensity along a direction perpendicular to the streaky pattern of the RHEED image. The data show five peaks corresponding to the parallel streaks in the RHEED image for the [11–20] orientation. The data start at the point of time ($t = 0$) where the GaN growth is initiated by opening the Ga shutter (the nitrogen shutter is always open as mentioned earlier). Since the growth is designed to be under the excess group III regime, as explained previously, the RHEED pattern is dim and diffuse. Thus, for initial times, the heights of these four peaks are small, and the background intensity is observed in the form of a broad peak. The parameter of interest is the height of the sharper peaks, and for simplicity of the calculation we have

chosen the second peak, centered around the distance of 200 pixels. The peak height is indicated by ΔI as shown in Fig. 3(a). At a time t_{close} , the Ga shutter is closed and the surface is exposed only to the active nitrogen. Subsequently, as the Ga layer gets thinner by being converted to GaN, the scattering is reduced and the peak height ΔI increases. At a time t_{cl} , the peak height is at its maximum and there is no further change. The parameter t_{cl} is, therefore, the time taken for the active nitrogen to consume the metallic layer on the growth surface and convert it to GaN.

A histogram of an image represents the number of pixels corresponding to each intensity level present in the image. RHEED images were obtained at more or less equal intervals from $t = 0$, when the deposition starts, to $t = t_{\text{cl}}$, when the excess metal has been consumed, and the corresponding histograms are presented in Fig. 3(b). There is a general distribution of intensity levels with a broad region starting from the intensity value of 0 and ending around 100. It can be observed that there is little overall change in the image except for the intensity level around $x = 105$ which significantly increases as the metallic layer is consumed by the active nitrogen and thus reduces in thickness and scattering probability. This peak corresponds to the sharp increase of brightness of the RHEED diffraction patterns. From Fig. 3(b), we can observe that this peak is initially very weak when the deposition takes place and both Ga and nitrogen shutters are open. When the growth is halted by closing the Ga shutter, this peak remains weak during 95% of the “clearing time” t_{cl} , after which there is a sudden increase in intensity. When the metallic layer has been consumed, this peak remains high as the RHEED pattern retains its brightness.

The RHEED evolution for the same growth sequence, consisting of deposition of GaN under excess Ga condition for 2 min (120 s) followed by the closing of the Ga shutter and subsequent exposure to the active nitrogen, has been analyzed by the two techniques described previously and compared in Fig. 4. In Fig. 4(a), the magnitude of pixel intensity peak, designated as ΔI [shown in Fig. 3(a)], is plotted as a function of time. When both Ga and nitrogen shutters are open, ΔI shows a low and nearly constant value. After the Ga shutter is closed, the value of ΔI remains low for a time and then sharply increases around 180 s. Figure 4(b) shows similar data derived from the histograms of Fig. 3(b). The number of pixels corresponding to $x = 105$, which is the region that shows a significant change during the growth process, is plotted with time. As in the case of Fig. 4(a), there is very little change in the level till $t \sim 180$ s, after which there is a sharp increase.

Both techniques discussed here provide similar information regarding the RHEED intensity variation with time and therefore either can be employed as a parameter for monitoring the growth. However, each has its own advantages and limitations. The RHEED intensity profile, that is the first technique, requires more process steps but has the advantage that minor extension of the code can also provide information regarding peak width and spacing, which traditionally has been employed to determine the film quality, strain, and composition. The second technique is simpler but may be dependent on the image quality and data acquisition parameters.

In this work, we have focused our effort on the single parameter, that is, the time required for the RHEED image to shift from a low contrast to a high contrast state after the deposition of a III-nitride film under excess group III for a certain period of time.

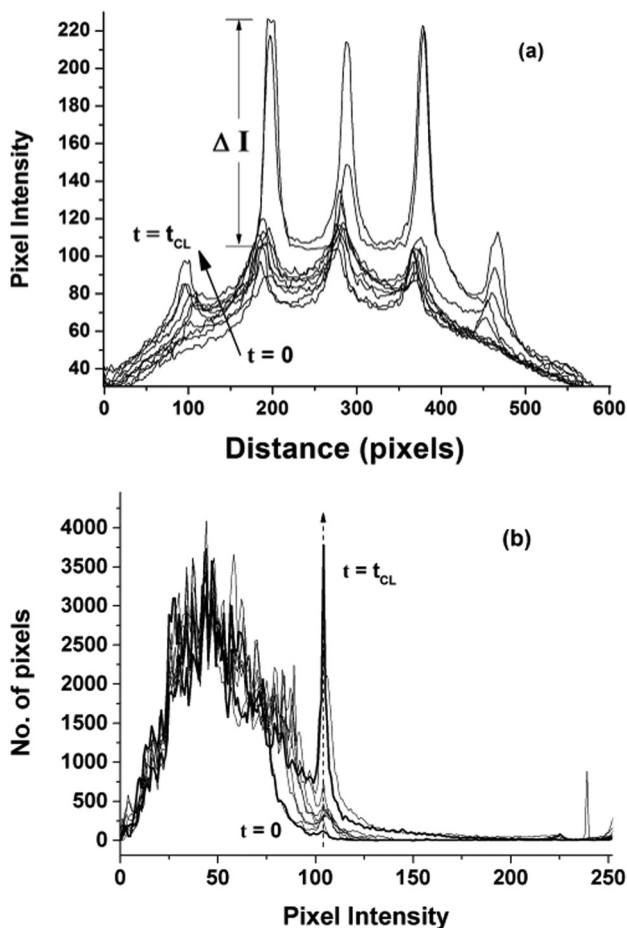


FIG. 3. RHEED image analysis: (a) plot profile and (b) histogram.

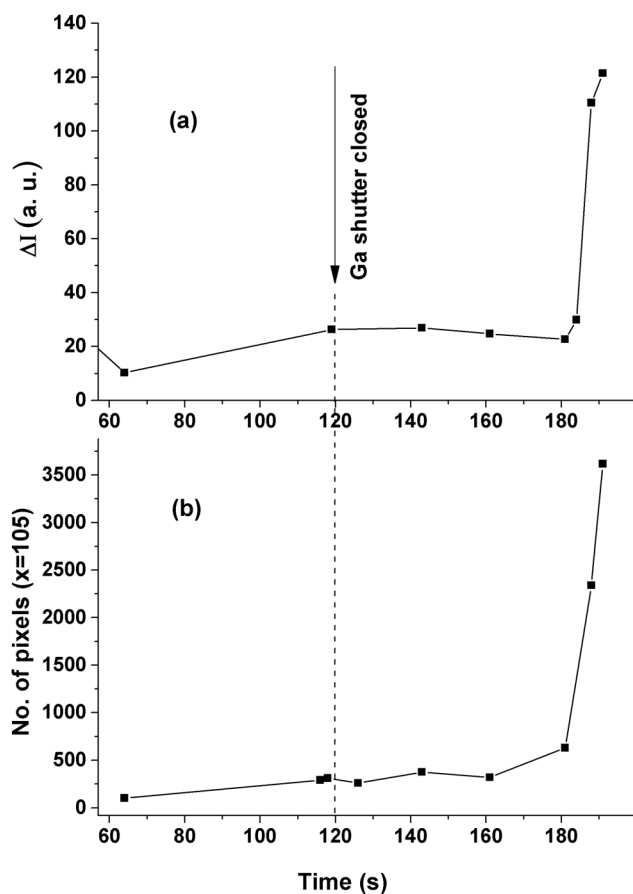


FIG. 4. RHEED transition times obtained from (a) plot profile and (b) histogram.

The growth rate, that is, the reaction rate, is controlled by the amount of active nitrogen reaching the sample surface under excess group III growth or by the amount of metal atoms present on the growth surface under excess group V conditions of growth. Therefore, during the period where both shutters are open and the growth occurs under excess group III conditions, the rate of increase of the build-up of the metallic layer depends on the quantitative value of the “excess,” that is, the number of metal atoms that remain unreacted per unit area per unit time. Thus, under the assumption that the desorption rate does not depend on the metal coverage, the metallic layer thickness increases with time in a linear fashion. Our initial results suggest that this is indeed true, within experimental limits, for short deposition times. At the point where the group III shutters are closed, a metal layer of a certain thickness T_m is present on the growth surface. This then reacts with the active nitrogen, and since there are no additional incoming group III atoms, the time for complete reaction of this metallic layer t_{cl} is directly proportional to the thickness of the layer. This technique, therefore, can be employed for an indirect but quantitative estimate of the “excess” of the group III to group V flux ratio, after appropriate calibration steps to determine the reaction rate of gallium

with the active nitrogen plasma, maintained under the same conditions of power, flow rate, and chamber pressure.

An important advantage of this technique is that it is independent of the effusion cell, substrate heater, or the active nitrogen RF source and so can be widely used. Finally, our method does not require expensive cameras, fast data acquisition systems, or complex data analysis and can be carried out in real time.

In order to benchmark our technique and to establish its effectiveness, we investigate four samples of GaN. They were grown under exactly the same conditions, i.e., effusion cell temperature, plasma power, nitrogen flow rate, pumping rate, etc., except for the substrate temperature. The samples S1, S2, S3, and S4 were grown at substrate temperatures of 800 °C, 790 °C, 780 °C, and 770 °C respectively.

The deposition of GaN depends on the arrival rate, the reaction rate, and the desorption rate of Ga, which is significant at the substrate temperatures used. As the deposition conditions are kept the same in all four cases, varying the substrate temperature will result in only a change in the desorption rate of Ga. At higher substrate temperatures, the desorption rate is expected to be higher, making the accumulated metallic film on the growth surface thinner.

The Ga shutter was kept open for exactly 120 s in each case, and then the metal shutter was closed and the excess metal on the surface was allowed to react with the nitrogen plasma. During the deposition times, due to the excess group III conditions of growth, metallic layers of different thicknesses were deposited on the surface. When the Ga shutter was closed, the consumption of excess Ga on the surface by the active nitrogen was initiated and this process was carried on till the entire amount was converted to GaN. During the time, since the scattering of electrons by the metallic film reduced, the RHEED pattern transformed from a dim and diffuse state to a clear and bright state.

In Fig. 5, ΔI (obtained from the plot profile) is plotted as a function of time for the four samples S1, S2, S3, and S4. For each sample, the plot of ΔI versus time can be divided into three distinct

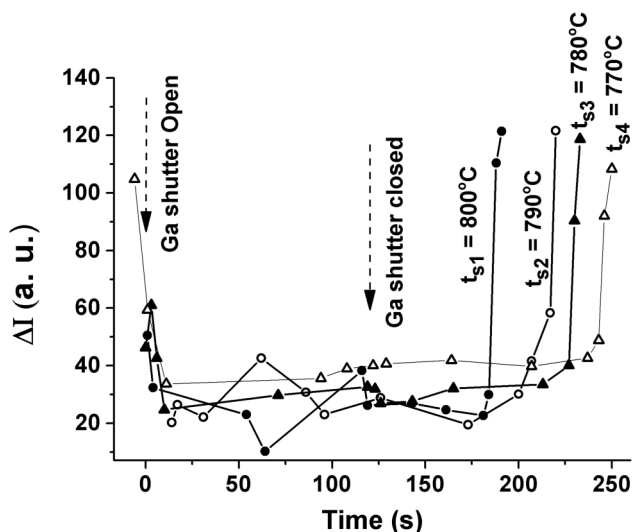


FIG. 5. RHEED transition times of GaN grown at different substrate temperatures.

regions. Initially, the value of ΔI is large, which falls drastically as soon as the Ga shutter is opened at time $t = 0$. For the next 120 s, the value of ΔI remains nearly constant within experimental error, at which point the Ga shutter is closed. Up to $t \sim 180$ s, no significant change in ΔI is seen for any of the four samples. After this point, the value of ΔI for sample S1, grown at a substrate temperature of 800 °C, increases sharply and reaches the maximum value within a few seconds. The times at which the values of ΔI increase sharply for samples S2, S3, and S4 are ~ 207 s, 227 s, and 243 s, respectively.

Therefore, we observe that for a lower substrate temperature, it requires a longer time for ΔI to increase. We have stated earlier that the desorption rate of Ga decreases with decreasing substrate temperature. Hence, at the end of Ga deposition for 120 s, the thickness of the accumulated metal layer increases progressively for samples S1–S4 as the substrate temperature is reduced. Since the time taken for the Ga layer to completely convert to GaN will be longer for thicker layers, i.e., for films deposited at lower substrate temperatures, our technique allows us to estimate the relative thickness of this metallic layer. For films grown at the same substrate temperature, our technique will directly indicate the relative group III/V flux ratios employed. Furthermore, these results also qualitatively establish the desorption rate of Ga at different substrate temperatures.

B. Extension of technique to AlGaN alloys

The analysis technique described in Sec. III A was extended to the growth of AlGaN alloys by PA-MBE. It should be noted that the alloy composition for AlGaN alloys under excess group III-rich conditions is controlled by the arrival rates of Al and the active nitrogen due to the very high sticking coefficient of Al and the strength of the Al–N bond. However, the optical and electrical properties of AlGaN alloys are controlled strongly by the presence of compositional inhomogeneities, which in turn depends on the group III (Ga + Al) to group V flux ratio. The growth is therefore typically carried out with excess gallium on the growth surface, which can act as a surfactant to smoothen the surface, as well as control the nanometer-scale potential fluctuations. Therefore, it is critical in this case to control excess gallium, and we have employed the *in situ* RHEED analysis technique described in Sec. III A. Growth of AlGaN alloys was carried out on to AlN buffer layers, under excess group III conditions, and the RHEED pattern as shown in Fig. 6(a) is dim and diffuse. The Al and Ga shutters were closed, and the surface was placed under active nitrogen to observe the evolution of the RHEED pattern. With the consumption of the excess metal, the RHEED transforms to that shown in Fig. 6(b), which has a much higher contrast. The analysis technique of obtaining the plot profile, that is, the spatial distribution of intensity along a direction perpendicular to the streaky pattern of the RHEED image, was applied to the RHEED images, and the results are shown in Fig. 6(c). A clear transition from a high contrast to a low contrast nature was obtained when growth was carried out under excess group III regime, and then when the metal shutters were closed the contrast levels slowly recovered.

It can be observed that even through the growth was carried out under excess group III conditions, the surface remains rough and faceted. This is partly due to a high AlN mole fraction being

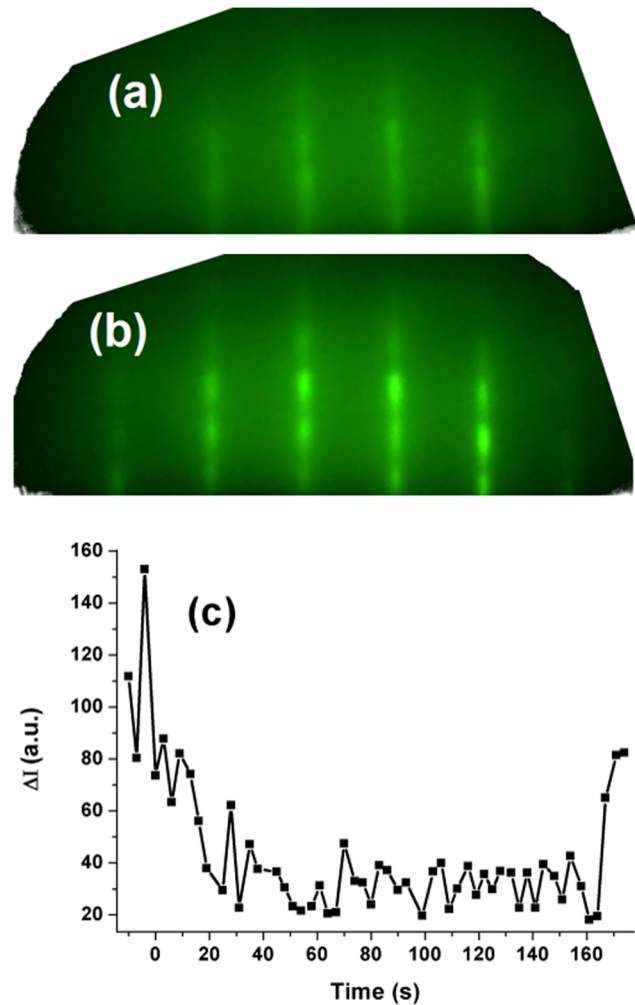


FIG. 6. RHEED image taken during AlGaN deposition (a), after reaction of the deposited metal with nitrogen plasma (b), and RHEED transition time obtained from the plot profile (c).

used in these alloys, which reduces the effectiveness of the gallium surfactant. The roughness can also be a result of the underlying layers, specifically the AlN buffer layer employed during initial stages of the growth. Our results indicate that the use of excess Al can lead to the growth of well oriented vertical nanorods. The presence of these structures shows itself in a diffuse background in the RHEED pattern, which does not modulate with the opening or closing of the metal shutters, and the contrast remains low. This can be a useful tool for detecting the presence of such nanostructures in an *in situ* real-time process. Such studies are, however, beyond the scope of the current paper and will be published elsewhere.

IV. SETUP FOR AN AUTOMATED GROWTH SYSTEM

The materials property of III-nitrides depends strongly on the Ga coverage on the growth surface, which can be estimated by the

technique described in this work. Since the acquisition and analysis can be performed in real time, this technique can be used to control the growth. The hardware driving the substrate rotation can be used to pinpoint the particular azimuthal angle corresponding to the appropriate RHEED pattern as shown in Fig. 2. The image can be acquired, analyzed, and the resultant value of ΔI can be used to determine the group III/V flux ratio. This value can be then used to modify the various growth parameters such as substrate temperature, effusion cell temperature or plasma power, and gas flow.

An alternative approach can be envisioned where a linear photosensor array can be directly attached to the RHEED fluorescent screen covering an area where one or more of the streaks appear. The intensity of the streaks and the region in between can be directly measured and compared. This will obviate the need for the RHEED video camera and associated hardware and software. This concept has been included in the schematic in Fig. 1.

V. CONCLUSIONS

Growth of AlGaIn alloys by PA-MBE has been carried out for a long time for its applications in both ultraviolet optoelectronic devices and high-power high-frequency devices. The group III/V flux ratio used during growth plays an extremely important role in determining the morphological, optical, and electrical properties of the sample. The group III/V flux ratio depends on a number of parameters and is difficult to calculate *a priori* or determine in real time. However, it is possible to monitor the RHEED pattern *in situ* and estimate the growth regime under which the ongoing growth is occurring and change growth parameters as necessary.

In this paper, we establish a technique for measurement of the RHEED intensity evolution with time following the deposition of a known thickness of GaN under excess group III conditions. The pattern, as measured by two different techniques, shows a sharp transition after a time t_{cl} . We establish that this time is a direct measure of the thickness of the metallic layer on the growth surface at the end of the deposition time and therefore the group III/V conditions employed. We further show that this technique can qualitatively predict the desorption rate of Ga with increasing substrate temperature. Finally, we extend the analysis technique to AlGaIn alloys.

We believe that this system will allow a low-cost addition of functionality of RHEED measurements for growth of III-nitride materials by PA-MBE.

ACKNOWLEDGMENTS

This work was partially funded by the Department of Information Technology [No. 12(3)/2011-PDD] and the Office of the Principal Scientific Advisor, Government of India (No. Prn SA/W-UV LED/2017). S.S. [No. 09/028 (0921)/2014-EMR-I] and A.D. [No. 09/028(0946)/2015-EMR-I] would like to acknowledge the Council of Scientific and Industrial Research Senior Research Fellowship (CSIR-SRF) scheme, C.S. (No. IF120257) would like

to acknowledge the Department of Science and Technology (DST) INSPIRE fellowship, A.S. would like to acknowledge the UGC Rajiv Gandhi National Fellowship scheme, and P.P. (No. PDF/2017/001605) would like to acknowledge the Science and Engineering Research Board (SERB) National Post-Doctoral Fellowship (NPDF) scheme for funding their work.

REFERENCES

- ¹N. Grandjean and J. Massies, *Appl. Phys. Lett.* **71**, 1816 (1997).
- ²H. Okumura, K. Balakrishnan, H. Hamaguchi, T. Koizumi, S. Chichibu, H. Nakanishi, T. Nagatomo, and S. Yoshida, *J. Cryst. Growth* **189/190**, 364 (1998).
- ³S. V. Ghaisas and A. Madhukar, *J. Vac. Sci. Technol. B* **3**, 540 (1985).
- ⁴D. Huang, P. Visconti, K. M. Jones, M. A. Reshchikov, F. Yun, A. A. Baski, T. King, and H. Morkoç, *Appl. Phys. Lett.* **78**, 4145 (2001).
- ⁵Z. Yang, L. K. Li, and W. I. Wang, *J. Vac. Sci. Technol. B* **14**, 2354 (1996).
- ⁶A. R. Smith, R. M. Feenstra, D. W. Greve, M.-S. Shin, M. Skowronski, J. Neugebauer, and J. E. Northrup, *Appl. Phys. Lett.* **72**, 2114 (1998).
- ⁷E. S. Hellman, *MRS Internet J. Nitride Semicond. Res.* **3**, 11 (1998).
- ⁸C. J. R. Sheppard and H. Ahmed, *Vacuum* **22**, 567 (1972).
- ⁹K. Britze and G. Meyer-Ehmsen, *Surf. Sci.* **77**, 131 (1978).
- ¹⁰B. Bölger and P. K. Larsen, *Rev. Sci. Instrum.* **57**, 1363 (1986).
- ¹¹J. S. Resh, K. D. Jamison, J. Strozier, and A. Ignatiev, *Rev. Sci. Instrum.* **61**, 771 (1990).
- ¹²M. Kneissl *et al.*, *Semicond. Sci. Technol.* **26**, 014036 (2011).
- ¹³J. Ferguson *et al.*, *Proc. SPIE* **2999**, 297 (1997).
- ¹⁴U. K. Mishra, P. Parikh, and Y. Wu, *Proc. IEEE* **90**, 1022 (2002).
- ¹⁵Y. Liao, C. Thomidis, C. Kao, and T. D. Moustakas, *Appl. Phys. Lett.* **98**, 081110 (2011).
- ¹⁶M. Misra, D. Korakakis, H. M. Ng, and T. D. Moustakas, *Appl. Phys. Lett.* **74**, 2203 (1999).
- ¹⁷J. Hwang, W. J. Schaff, L. F. Eastman, S. T. Bradley, L. J. Brillson, D. C. Look, J. Wu, and W. Walukiewicz, *Appl. Phys. Lett.* **81**, 5192 (2002).
- ¹⁸A. Bhattacharyya, W. Li, J. Cabalu, T. D. Moustakas, D. J. Smith, and R. L. Hervig, *Appl. Phys. Lett.* **85**, 4956 (2004).
- ¹⁹S. Matta, J. Brault, M. Korytov, T. Q. P. Vuong, C. Chaix, M. A. Khalifioui, P. Vennéguès, J. Massies, and B. Gil, *J. Cryst. Growth* **499**, 40 (2018).
- ²⁰P. Pramanik, S. Sen, C. Singha, A. S. Roy, A. Das, S. Sen, and A. Bhattacharyya, *J. Appl. Phys.* **120**, 144502 (2016).
- ²¹E. J. Tarsa, B. Heying, X. H. Wu, P. Fini, S. P. DenBaars, and J. S. Speck, *J. Appl. Phys.* **82**, 5472 (1997).
- ²²S. Rouvimov *et al.*, *Mater. Res. Soc. Symp. Proc.* **1741**, mrsf14-1741-aa04-04 (2015).
- ²³A. V. Sampath, G. A. Garrett, C. J. Collins, W. L. Sarney, E. D. Readinger, P. G. Newman, H. Shen, and M. Wraback, *J. Electron. Mater.* **35**, 641 (2006).
- ²⁴C. Singha, S. Sen, P. Pramanik, M. Palit, A. Das, A. S. Roy, S. Sen, and A. Bhattacharyya, *J. Cryst. Growth* **481**, 40 (2018).
- ²⁵S. D. Burnham and W. A. Doolittle, *J. Vac. Sci. Technol. B* **24**, 2100 (2006).
- ²⁶S. D. Burnham, W. Henderson, and W. A. Doolittle, *Phys. Status Solidi C* **5**, 1855 (2008).
- ²⁷D. F. Storm, M. T. Hardy, D. S. Katzer, N. Nepal, B. P. Downey, D. J. Meyer, T. O. McConkie, L. Zhou, and D. J. Smith, *J. Cryst. Growth* **456**, 121 (2016).
- ²⁸C. Wu *et al.*, *Cryst. Growth Des.* **16**, 5023 (2016).
- ²⁹I. Susanto, T. Tsou, Z. Yang, C. Lee, H. Li, and I. Yu, *J. Alloys Compd.* **710**, 800 (2017).